Layered Polyline Drawings of Planar Graphs

Debajyoti Mondal
Department of Computer Science, University of Saskatchewan, Saskatoon, Canada

Abstract

A k-layer polyline drawing of a planar graph G is a planar drawing of G on a set L of k parallel lines such that each vertex is mapped to a point on L and each edge is mapped to a polygonal chain with the endpoints and bends lying on L. In the fixed embedding setting, the output drawing maintains the given planar embedding, whereas in the variable embedding setting, the embedding may change. Every n-vertex planar graph admits a polyline drawing on $2n/3$ layers, which is the best known upper bound for both settings. We improve this bound in the variable embedding setting. We show that every planar graph can be drawn on $14n/27 + O(\sqrt{n})$ layers by choosing a proper planar embedding, breaking the long-standing $2n/3$-layer barrier.

2012 ACM Subject Classification Mathematics of computing → Discrete mathematics

Keywords and phrases Layered Drawing, Variable Embedding, Polyline Drawing, Cycle Separator

Digital Object Identifier 10.4230/LIPIcs.GD.2025.34

Acknowledgements The research is supported in part by the Natural Sciences and Engineering Research Council of Canada (NSERC).

1 Introduction

A *polyline drawing* of a planar graph G maps each vertex of G to a distinct point in the Euclidean plane, and each edge of G to a polygonal chain such that no two edges cross except possibly at their common endpoints. A *straight-line drawing* is a special case of polyline drawing where every polygonal chain is a straight line segment. The *area* of a drawing Γ is the area of the smallest axis-aligned rectangle R that encloses Γ. The *width* and *height* of Γ are the width and height of R, respectively. Since a drawing can be scaled down arbitrarily, to measure the area we often require Γ to be a *grid drawing*, i.e., a drawing where all the vertices and bends have integer coordinates.

Drawing planar graphs on a small integer grid is an active research area in graph drawing [5, 6, 11, 13, 16, 27, 22, 25]. In this paper we focus on layered polyline drawings that attempt to reduce the height of the drawing while the other dimension could be unbounded. This can be seen as a drawing of a graph on a set of parallel lines or layers. Formally, a *k-layer polyline drawing* of a planar graph G is a planar drawing of G on a set L of k parallel lines (i.e., *layers*) such that each vertex is mapped to a point on L and each edge is mapped to a polygonal chain with the endpoints and bends lying on L. This drawing model has been studied extensively in the literature [4, 14, 17, 24, 26]. The distances between consecutive layers in a layered drawing can be assumed to be one unit, as any drawing with non-uniform spacing can be modified to satisfy this property without increasing the number of layers [17] (e.g., by adding extra bend points on edges at their intersections with layers and adjusting the gaps between layers). The results on the grid drawing of planar graphs readily imply upper bounds on the number of layers for their layered drawings. We briefly review these results under two drawing models. One is the *fixed embedding setting*, where the output drawing must respect the input planar embedding (i.e., a fixed combinatorial embedding with a prescribed outer face), and the other is the *variable embedding setting*, where the embedding in the output drawing can be different from the input embedding.

33rd International Symposium on Graph Drawing and Network Visualization (GD 2025).
Editors: Vida Dujmović and Fabrizio Montecchiani; Article No. 34; pp. 34:1–34:10
Leibniz International Proceedings in Informatics
LIPICS Schloss Dagstuhl – Leibniz-Zentrum für Informatik, Dagstuhl Publishing, Germany

Fixed Embedding Setting. Every n-vertex planar graph admits a straight-line grid drawing with $O(n^2)$ area [11, 25]. Many algorithms have appeared in the literature that compute straight-line drawings [8, 9] and polyline drawings [6, 29] of planar graphs, where one dimension of the drawing (equivalently, number of layers) is bounded by $2n/3$. To provide an upper bound on area, drawing algorithms are typically presented on *maximal planar graphs* or *planar triangulations*, where each face of the given embedding is a cycle of three vertices. Similarly, throughout the paper, we will consider the input to be a planar triangulation. This upper bound on the number of layers is tight, that is, every polyline drawing of an n-vertex nested triangles graph requires at least $\lfloor 2(n-1)/3 \rfloor$ layers [6].

Variable Embedding Setting. The upper bound of $2n/3$ layers implied by the results in the fixed embedding setting [8, 6, 28] applies also to the variable embedding setting. To the best of our knowledge, it is not known whether a better bound can be achieved for arbitrary planar graphs in the variable embedding setting. However, better upper bounds are known in the variable embedding setting for several subclasses of planar graphs (e.g., outerplanar graphs [3], series-parallel graphs [31, 30], planar graphs with small maximum degree or small cycle separator [17], planar 3-trees [21, 20], and nested triangles graphs [18]). The best known lower bound on layers in the variable embedding setting is $\lfloor n/3 - 1 \rfloor$ [18]. The large gap between the upper and lower bounds motivates this paper.

Our Contribution. We develop an algorithm that can draw arbitrary n-vertex planar graphs on $14n/27 + O(\sqrt{n})$ layers in the variable embedding setting. The idea is to use a balanced cycle separator of size $O(\sqrt{n})$ to decompose the input planar graph into two subgraphs. We draw these subgraphs separately such that they can be merged without adding too many additional layers. The main challenge appears to be computing careful positions of the separator vertices in both drawings such that during the merge step, the vertices can be aligned with small modification. We tackle this by designing a drawing method that allows flexible positioning of separator vertices with necessary visibilities.

Note that the technique of using a separator to decompose a graph into subgraphs and then to merge the drawing of the subgraphs to obtain a drawing has previously been used in the literature [31, 15]. In particular, Durocher and Mondal [15] used a cycle separator of size $\lambda \in O(\sqrt{n})$ to draw an n-vertex planar graph in $4n/9 + O(\lambda\Delta)$ layers, where Δ is the maximum degree in the graph. If $\Delta \in o(\sqrt{n})$, the bound becomes $4n/9 + o(n)$ layers, but for $\Delta \geq \sqrt{n}$, it can become larger than n layers. When drawing each subgraph in $4n/9$ layers, their strategy was to contract the rest of the graph into a single vertex. However, the merge step required rerouting the edges incident to the separator vertices, which added an additional $O(\lambda\Delta)$ layers. Later, they used an edge separator of size $\lambda' \in O(\sqrt{n\Delta})$ instead of a cycle separator to improve the bound to $4n/9 + O(\lambda')$ [17]. However, both these additive terms $O(\lambda\Delta)$ and $O(\lambda')$ can sometimes be large (e.g., consider a wheel graph), and the total layer count may exceed n.

2 Preliminaries

A planar graph G is called *maximal* if the addition of any more edges to G results in a non-planar graph. Let Γ be a straight-line drawing of a maximal planar graph in $\mathbb{R}^2$. Then every face in Γ corresponds to a triangle in $\mathbb{R}^2$, and hence the graph is also called a *planar triangulation*. A planar graph is called *internally triangulated* if every inner face is a cycle of length three. A simple cycle C of G is called a *cycle separator* if both the interior and exterior

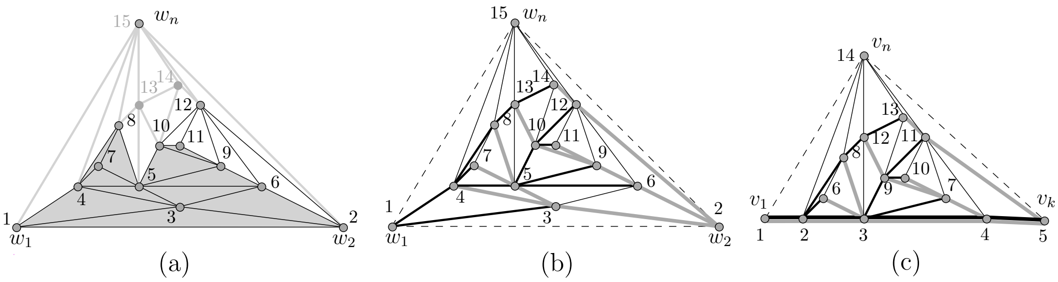

Figure 1 (a) Illustration for a canonical ordering. The graph G_{11} lies in the shaded region. (b) Corresponding Schnyder realizer. (c) Illustration for a Schnyder realizer of H.

of C contain at most $2n/3$ vertices. Every planar graph admits a simple cycle separator of size $O(\sqrt{n})$ and several studies attempt to improve the constant factor [12, 19, 23]. Throughout the paper we assume that the layers are horizontal and denote the x- and y-coordinates of a vertex v by $x(v)$ and $y(v)$, respectively.

Canonical Ordering and Schnyder Realizer. Let G be a planar triangulation, and let w_1, w_2 and w_n be the outer vertices of G in counter-clockwise order. Let $\sigma = (w_1, w_2, ..., w_n)$ be an ordering of all vertices of G. We denote by G_k, $3 \le k \le n$, the subgraph of G induced by $\{w_1, w_2, \ldots, w_k\}$, and by P_k, the clockwise path on the outer face of G_k that starts at w_1 and ends at w_2. The ordering σ is called a *canonical ordering* of G with respect to the outer edge (w_1, w_2) if for each k, $3 \le k \le n$, the following two conditions are satisfied [11]:

(a) G_k is 2-connected and internally triangulated.

(b) If $k+1 \le n$, then w_{k+1} is an outer vertex of G_{k+1} and the neighbors of w_{k+1} in G_k appear consecutively on P_k.

For a vertex w_{k+1}, let P_k be the outer path $w_1, \ldots, w_l, \ldots, w_r, \ldots, w_2$ of G_k, where w_l and w_r are the leftmost and rightmost neighbors of w_{k+1}, respectively. We call the edges (w_l, w_{k+1}) and (w_{k+1}, w_r) the *l-edge* and the *r-edge* of w_{k+1}, respectively. The other edges incident to w_{k+1} in G_k are called the *m-edges* of w_{k+1}. For example, in Figure 1(a), the edges $(w_{12}, w_{10}), (w_{12}, w_2)$ are respectively the l-edge and r-edge of w_{12}. The m-edges of w_{12} are $(w_{12}, w_{11}), (w_{12}, w_9)$ and (w_{12}, w_6). The set of all m-edges in G corresponds to a tree T_m, which is rooted at w_n and spans all the inner vertices. Figure 1(b) illustrates T_m in thin solid lines. Similarly, the set of l-edges in G except (w_1, w_n) and (w_1, w_2) corresponds to a tree rooted at w_1, and the set of r-edges except (w_2, w_n) and (w_1, w_n) is a tree rooted at w_2. Figure 1(b) depicts the trees T_l and T_r in thick black and thick gray edges, respectively. The trees $\{T_l, T_r, T_m\}$ form the *Schnyder realizer* [25] of G. Each of T_l, T_r and T_m corresponds to a canonical ordering of G. Let $\mathrm{leaf}(T_l), \mathrm{leaf}(T_r)$ and $\mathrm{leaf}(T_m)$ be the number of leaves in T_l, T_r and T_m, respectively.

▶ **Lemma 1** (Bonichon et al. [7]). *Let $\{T_l, T_r, T_m\}$ be a minimum Schnyder realizer of an n-vertex triangulation. Then $\mathrm{leaf}(T_l) + \mathrm{leaf}(T_r) + \mathrm{leaf}(T_m) = 2n - \Delta$, where Δ is the number of cyclic inner faces in the realizer.*

Generalization to Internally Triangulated Graphs. The notions of canonical ordering and Schnyder realizer have been extended to other classes of planar graphs that are not necessarily triangulated [1, 2]. However, to describe our algorithm in this paper, we only need to consider the 2-connected and internally triangulated graphs. Let H be a 2-connected and internally triangulated graph with the outer vertices $v_1, \ldots, v_k, v_n$ in counter-clockwise order. If $k > 2$, then consider a dummy edge (v_1, v_k) and triangulate the face $v_1, \ldots, v_k, v_1$. We can now order the inner vertices of H satisfying properties (a) and (b) of a canonical ordering. We can define the l- and r-edges in the same way as we defined for canonical ordering. Observe that the set of m-edges corresponds to a tree T_m, which is rooted at v_n, but the l-edges and r-edges may no longer form the trees T_l and T_r. To form the trees T_l and T_r, we assume the edges on the outer path $v_1, v_2, \ldots, v_k$ to belong to both these trees, e.g., Figure 1(c). Let Γ be a drawing of H. We call a vertex v of H to have *top visibility* in Γ if the vertically upward ray starting at v does not intersect Γ except at v.

We now have the following lemma, which will be used later to describe our drawing algorithm.

▶ **Lemma 2.** *Let H be a 2-connected and internally triangulated graph with the outer vertices $v_1, \ldots, v_k, v_n$ in counter-clockwise order. Let T_l, T_r, T_m be a Schnyder realizer of H rooted at v_1, v_k, v_n, respectively, where $v_1, \ldots, v_k$ is a path in both T_l and T_r. Then H admits the following types of layered drawings:*

(a) *A drawing on $\mathrm{leaf}(T_l)$ layers where the path $v_1, \ldots, v_k$ is drawn on the bottommost layer and v_1, v_k have top visibility.*

(b) *A drawing on $\mathrm{leaf}(T_r)$ layers where the path $v_1, \ldots, v_k$ is drawn on the bottommost layer and v_1, v_k have top visibility.*

(c) *A drawing on $\mathrm{leaf}(T_m) + k$ layers where the path $v_1, \ldots, v_k$ lies along a vertical line L (perpendicular to the layers) and all other vertices and edges lie in the same half-plane of L.*

Proof. Here we show that H admits a drawing on a $(\mathrm{leaf}(T_m) + k) \times \mathrm{leaf}(T_l)$ grid where the path $v_1, \ldots, v_k$ is drawn on the bottommost layer and v_1, v_k has top visibility. This will correspond to the type-(a) drawing of the lemma, whereas the type-(c) drawing can be obtained by rotating the drawing 90°. To obtain the drawing of type-(b), one can construct drawing on a $(\mathrm{leaf}(T_m) + k) \times \mathrm{leaf}(T_r)$ grid symmetrically.

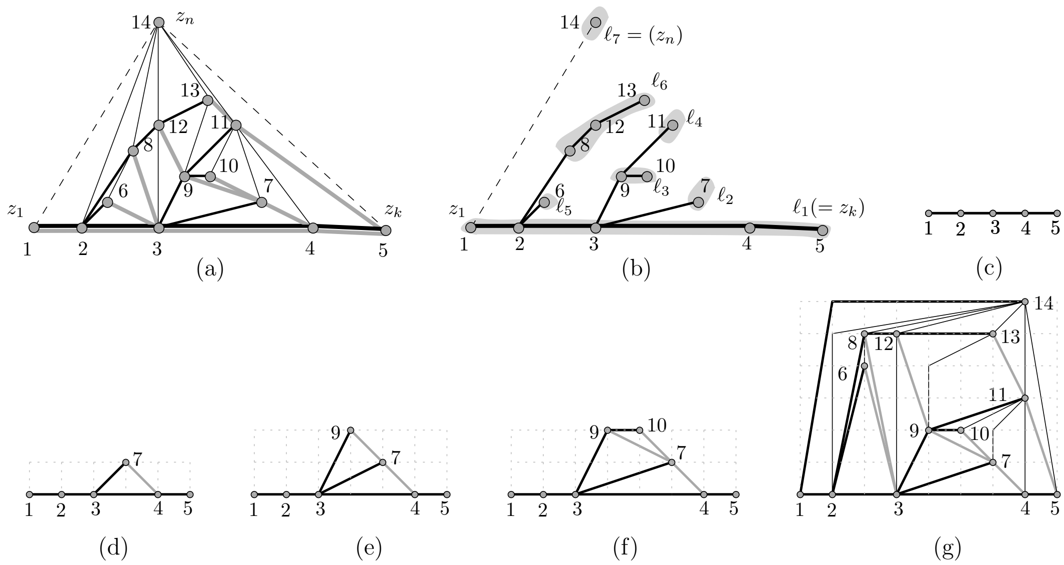

Figure 2 (a) A planar graph H. (b) Pseudo-segments of T_l are shaded in gray. (c)–(f) Illustration for some vertex insertions in the order they appear in σ. (g) The final polyline drawing of H.

We assume familiarity with the "shift algorithm" to compute grid drawings for planar graphs [11]. We treat the vertex v_n as a leaf of T_l. Let $z_1(= v_1), \ldots, z_k(= v_k)$, $z_{k+1}, \ldots,$ $z_n(= v_n)$ be the vertices listed according to a preorder traversal of T_l, where the children are visited in counter-clockwise order. Then the ordering $\sigma = (z_{k+1}, \ldots, z_n)$ is another canonical ordering of G [10, Lemma 3.5]. Let $\ell_1(= z_k), \ell_2, \ldots, \ell_s(= z_n)$ be the leaves of T_l according to the preorder traversal of T_l, where s is the number of leaves in T_l. We assign each leaf of T_l a path called *pseudo-segment*, as follows. The first *pseudo-segment* $\mathcal{S}_1$ *assigned to* ℓ_1 is the unique path from z_1 to $l_1(= z_k)$. The *pseudo-segment* $\mathcal{S}_j$ *assigned to* ℓ_j, where $1 < j \leq s$, is the shortest path in T_l that starts at ℓ_j and ends at a vertex which is adjacent to some previous pseudo-segment. Figure 2(a)–(b) illustrates such a pseudo-segment decomposition of T_l. Let H_q be the subgraph of H induced by the vertices $z_1, \ldots, z_q$, where $1 \leq q \leq n$. We now show that H_q admits a drawing Γ_q satisfying the following properties.

- $\boldsymbol{I_1}$. Γ_q is a polyline drawing on $(\delta + k) \times j$ layers, where δ is the number of leaves of T_m in H_q and z_q belongs to the pseudo-segment $\mathcal{S}_j$.
- $\boldsymbol{I_2}$. The y-coordinates of the vertices of a pseudo-segment $\mathcal{S}_i$ is i, where $1 \leq i \leq j$.
- $\boldsymbol{I_3}$. The clockwise path P_q on the outer face of H_q is drawn as a strictly x-monotone polygonal chain in Γ_q, i.e., the vertices on P_q have top visibility.

We first draw the path $z_1(= v_1), \ldots, z_k(= v_k)$ by placing each z_i, where $1 \leq i \leq k$, at $(i, 1)$ (Figure 2(c)). It is straightforward to verify I_1–I_3 for Γ_k. We now add the remaining vertices in the order they appear in σ. While inserting a new vertex z_t, where $t > k$, we consider two cases depending on whether z_t is a leaf or an internal vertex in T_m. Let $P_t = (z_1, \ldots, z_t^l, z_t, z_t^r, \ldots, z_k)$ be the clockwise path on the outer face of H_t. Let $\mathcal{S}_{j'}$ be the pseudo-segment that contains z_t.

Case 1. If z_t is a leaf of T_m, then we shift the vertices $z_t^r, \ldots, z_k$ and their descendants in T_m one unit to the right, e.g., see the vertex insertions in Figure 2(d)–(f). Then we place z_t at $(x(z_t^r) - 1, j')$. Note that z_t^l and z_t^r have top visibility in Γ_{t-1} and retain this visibility even after the shift. Since j' is the highest y-coordinate in the current drawing and since $x(z_t) = x(z_t^r) - 1$, we can draw the edge (z_t^r, z_t) with a straight line segment without introducing any edge crossing. If z_t^l belongs to $\mathcal{S}_{j'}$ or if $x(z_t) = x(z_t^l) + 1$, then we can draw (z_t, z_t^r) with a straight line segment. Otherwise, we use a bend point at $(x(z_t^l) + 1, j')$.

We now show that Γ_t satisfies properties I_1–I_3. Here I_1 holds as the drawing width increases by one unit due to the insertion of a new leaf and the height of the drawing becomes j'. The shift operation keeps the resulting drawing planar, does not change the y-coordinates of the vertices, and does not affect the x-monotonicity of the edges [11]. Therefore, the drawing of the l- and r-edges of z_t ensures that the path (z_t^l, z_t, z_t^r) is drawn as an x-monotone polygonal chain where the vertices z_t^l, z_t, z_t^r have top visibility. Consequently, the drawing Γ_t satisfies I_2 and I_3.

Case 2. If z_t is an internal vertex of T_m, then we place z_t at $(x(z_t^r) - 1, j')$. Let (z_t, z') be the first m-edge of z_t in clockwise order. Since P_{t-1} is strictly x-monotone in Γ_{t-1}, the other vertices on the pseudo-segment $\mathcal{S}_{j'}$ before z_t lie to the left of the line $x = x(z')$. Since z' is a child of v in T_m, it cannot belong to $\mathcal{S}_{j'}$ and hence its y-coordinate is smaller than j'. Hence the grid point $(x(z_t^r) - 1, j')$ is empty.

Since $x(z_t) = x(z_t^r) - 1$, we can draw (z_t, z_t^r) with a straight line segment (e.g., insertion of z_{14} in Figure 2(g)). If z_t^l belongs to $\mathcal{S}_{j'}$ or if $x(z_t) = x(z_t^l) + 1$, then we can draw (z_t, z_t^l) with a straight line segment. Otherwise, we use a bend point at $(x(z_t^l) + 1, j')$ (Figure 2(g)). We now consider the drawing of the m-edges. To draw an m-edge (z_t, w), we first check whether $y(w) = j' - 1$. If so, then we can draw the edge with a straight line segment. Otherwise, we create a bend point at $(x(w), j'-1)$. This is possible because w appears in a pseudo-segment $\mathcal{S}_{j''}$ where $j'' < j$, and thus the grid point $(x(w), j'-1)$ is empty. Here I_1 holds as we do not change the width of the current drawing and the height increases only when we start adding a new pseudo-segment. I_2–I_4 hold by the drawing of the l- and r-edges of z_t ensuring the top visibility for z_t^l, z_t, z_t^r, and by the property of the shift algorithm that it preserves the y-coordinates of the vertices and the x-monotonicity of the edges [11]. ◀

3 Drawing Algorithm

We first choose a suitable embedding of G, then decompose the graph into two subgraphs and draw them independently, and finally, merge these drawings by considering different cases depending on the structure of their Schnyder realizers.

Embedding Selection. Let G be a planar triangulation with a simple cycle separator $C = (v_1, \ldots, v_k)$ of size $k = O(\sqrt{n})$, as shown in bold in Figure 3(a). Let Γ be a planar embedding of G and let (a, b, c) be an inner face in Γ such that $(a, b) = (v_1, v_k)$ is an edge of C and c is an inner vertex in Γ. We then create a new planar embedding Γ' by choosing (a, b, c) as the outer face (Figure 3(b)). We then add a subdivision vertex d on the edge (a, b) (Figure 3(c)), and triangulate the inner face incident to d. Finally, for each pair of vertices v_i, v_j in C, where $1 \le i+1 < j \le k$, if the edge (v_i, v_j) exists in G, then we add a subdivision vertex on (v_i, v_j) and triangulate the graph. Let G' be the resulting drawing. By G_i (G_o) we refer to the subgraph of G' that lies in the closed interior (exterior) of C. By n_o and n_i we refer to the number of vertices of G_o and G_i, respectively. Since we added at most $O(\sqrt{n})$ division vertices, $n_o, n_i \le 2n/3 + O(\sqrt{n})$.

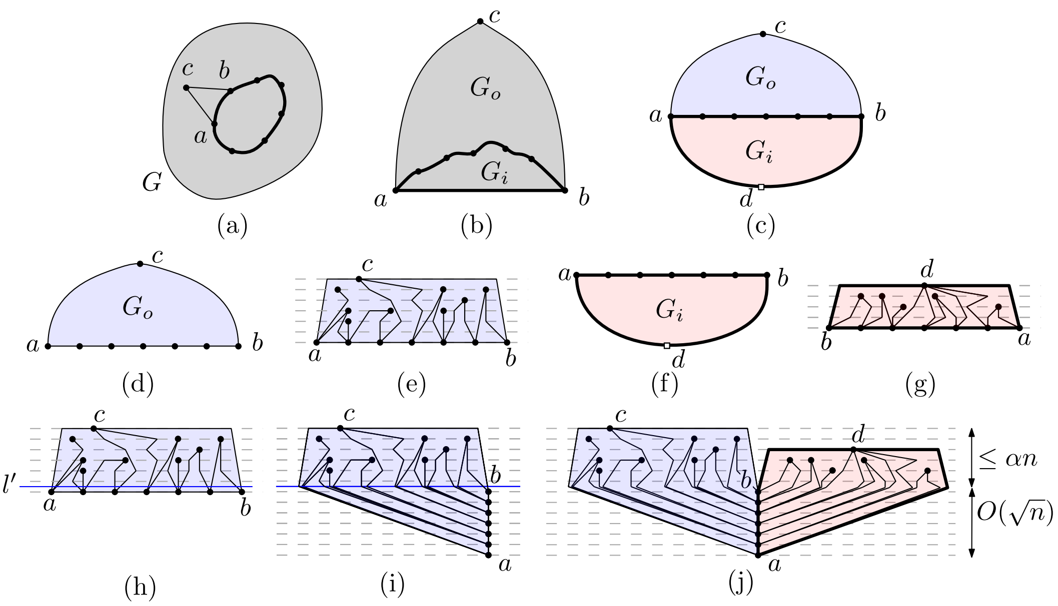

Figure 3 (a) A planar graph G with a cycle separator shown in bold. (b) Computation of the required embedding. (c) An illustration for G'. (d)–(e) A drawing of G_o, where only a few edges adjacent to the vertices of $a, \ldots, b$ are shown. (f)–(g) A drawing of G_i. (h)–(i) Modification of the drawing of G_o. (j) The final drawing of G' obtained by merging the drawings of G_o and G_i.

Draw and Merge. Let T_l^o, T_r^o, T_m^o be the trees of a minimum Schnyder realizer of G_o rooted at a, b, c, respectively. Similarly, let T_l^i, T_r^i, T_m^i be the trees of a minimum Schnyder realizer of G_i rooted at b, a, d, respectively. Let $\alpha \in (0, 2/3]$ be a positive constant to be determined later. We now consider two cases depending on whether the following condition holds: $\min\{\text{leaf}(T_l^o), \text{leaf}(T_r^o)\} \le \alpha n$ and $\min\{\text{leaf}(T_l^i), \text{leaf}(T_r^i)\} \le \alpha n$.

Case 1 ($\min\{\text{leaf}(T_l^o), \text{leaf}(T_r^o)\} \le \alpha n$ and $\min\{\text{leaf}(T_l^i), \text{leaf}(T_r^i)\} \le \alpha n$). In this case we construct a drawing of G' on $\alpha n + O(\sqrt{n})$ layers, as follows. By Lemma 2, G_o admits a drawing on $\min\{\text{leaf}(T_l^o), \text{leaf}(T_r^o)\} \le \alpha n$ layers with the path $v_1(=a), v_2, \ldots, v_k(=b)$ of the cycle separator drawn on the bottommost layer (Figure 3(d)–(e)). Let l_0 be the bottommost layer and let l_1 be the layer above l_0. We consider a horizontal line l' between these two layers (i.e., the blue line in Figure 3(h)) and add a bend point at each intersection point between l' and the edges. We insert $k-1$ layers below l_0 and move the vertices $v_{k-1}, \ldots, v_2, v_1(=a)$ on these newly inserted layers consecutively below b, as shown in Figure 3(h)–(i). We redraw the edges and part of the edges below l' with straight line segments. Since the ordering of the bend points on l' corresponds to the ordering of the vertices $a, \ldots, b$ in the newly inserted layers, the resulting drawing remains planar. Since $k+1 = O(\sqrt{n})$, the drawing takes at most $\alpha n + O(\sqrt{n})$ layers. We draw G_i using Lemma 2 on $\min\{\text{leaf}(T_l^i), \text{leaf}(T_r^i)\} \le \alpha n$ layers with the path $v_1(=a), v_2, \ldots, v_k(=b)$ of the cycle separator drawn on the bottommost layer (Figure 3(f)–(g)). We then modify the drawing to bring the vertices $v_{k-1}, \ldots, v_1(=a)$ on a set of $(k-1)$ consecutive bottommost layers of the drawing below b. To obtain the final drawing of G', we bring the drawings of G_o and G_i close together such that they coincide on the path $a, \ldots, b$ (Figure 3(j)). The top visibility of b ensures planarity, i.e., the polylines representing (c, b) and (d, b) do not overlap. Since these drawings share a common set of layers, the number of layers is bounded by $\alpha n + O(\sqrt{n})$.

Case 2 ($\min\{\text{leaf}(T_l^o), \text{leaf}(T_r^o)\} > \alpha n$ or $\min\{\text{leaf}(T_l^i), \text{leaf}(T_r^i)\} > \alpha n$). Without loss of generality assume that $\min\{\text{leaf}(T_l^o), \text{leaf}(T_r^o)\} > \alpha n$. Then by Lemma 1, we have $\text{leaf}(T_m^o) \le 2n_o - 2\alpha n$. In this scenario, we consider two subcases depending on whether $\text{leaf}(T_m^i) \le 2n_i/3$ or not, and in both cases we construct a drawing of G' on $2n_o - 2\alpha n + O(\sqrt{n}) + 2n_i/3$ layers.

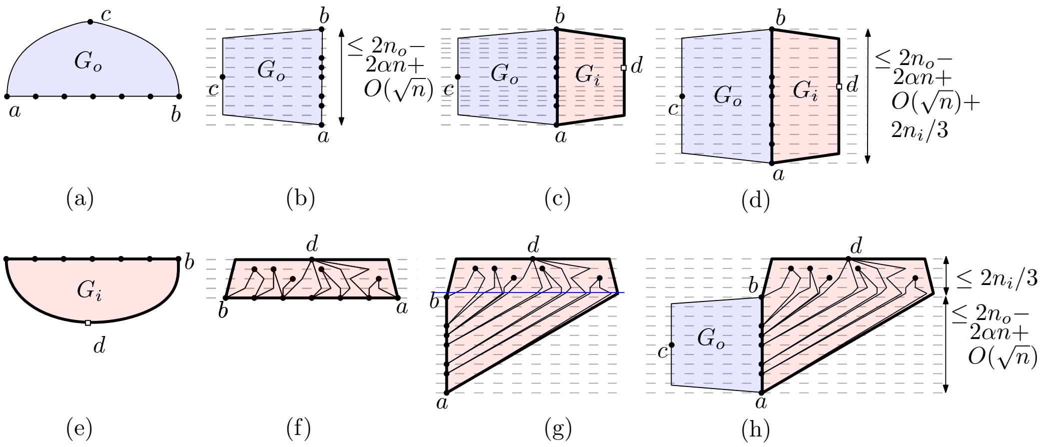

Figure 4 Illustration for (a)–(d) Case 2.1 and (e)–(h) Case 2.2.

Case 2.1 (leaf$(T^i_m) \le 2n_i/3$). We first draw G_o using Lemma 2 in leaf$(T^o_m) + k \le 2n_o - 2\alpha n + O(\sqrt{n})$ layers where the path $v_1, \ldots, v_k$ is drawn along a vertical line L (perpendicular to the layers) and the drawing lies to the left half-plane of L (Figure 4(a)–(b)). We now draw G_i on the right half-plane of L taking the drawing of $v_1, \ldots, v_k$ as input, and inserting the remaining vertices of G_i following the method described in the proof of Lemma 2. This inserts new layers within the drawing of G_o. Since leaf$(T^i_m) \le 2n_i/3$, the total number of layers remains bounded by $2n_o - 2\alpha n + O(\sqrt{n}) + 2n_i/3$ (Figure 4(c)–(d)).

Case 2.2 (leaf$(T^i_m) > 2n_i/3$). We draw G_o in the same way as in Case 2.1 on $2n_o - 2\alpha n + O(\sqrt{n})$ layers. By Lemma 1, either leaf(T^i_l) or leaf(T^i_r) is at most $2n_i/3$. By Lemma 2, G_i admits a drawing on $2n_i/3$ layers with the path $v_1(= a), v_2, \ldots, v_k(= b)$ drawn on the bottommost layer l_0 (Figure 4(e)–(f)). We modify the drawing similar to Case 1 by inserting new layers below l_0 and moving the vertices $v_{k-1}, \ldots, v_1(= a)$ below b. However, instead of placing these vertices on consecutive layers, we move them to their corresponding layers in the drawing of G_o. Hence the total number of layers after merging the drawings of G_o and G_i is bounded by $2n_o - 2\alpha n + O(\sqrt{n}) + 2n_i/3$ (Figure 4(g)–(h)).

Upper Bound Computation. The algorithm produces a drawing on $\max\{\alpha n + O(\sqrt{n}), 2n_o - 2\alpha n + O(\sqrt{n}) + 2n_i/3\}$ layers. Since $n_o + n_i = n + O(\sqrt{n})$ and $n_o \le 2n/3 + O(\sqrt{n})$, we have

$$\begin{aligned}
2n_o - 2\alpha n + O(\sqrt{n}) + 2n_i/3 &= 2(n_o + n_i)/3 + 4n_o/3 - 2\alpha n + O(\sqrt{n}) \\
&\le 2n/3 + 8n/9 - 2\alpha n + O(\sqrt{n}) \\
&\le 14n/9 - 2\alpha n + O(\sqrt{n}).
\end{aligned}$$

Hence the number of layers is bounded by $\max\{\alpha n + O(\sqrt{n}), 14n/9 - 2\alpha n + O(\sqrt{n})\}$ layers, which is minimized when $\alpha = 14/27$. We thus have the following theorem.

▶ **Theorem 3.** *Every planar graph with n vertices admits a planar polyline drawing on $14n/27 + O(\sqrt{n})$ layers.*

4 Conclusion

In this paper we have shown how to draw an n-vertex planar graph using $14n/27 + O(\sqrt{n})$ layers. Since only a $\lfloor n/3 - 1 \rfloor$ lower bound is known [18], a natural open problem is to reduce this gap. It would be interesting to investigate whether our strategy can be combined with the techniques in [15, 17] to improve the upper bound further.

We did not analyze the number of bends produced in our drawing, which could be another parameter for optimization. The trade-off between the number of layers and the number of bends also requires further investigation.

References

1 Luca Castelli Aleardi, Éric Fusy, and Thomas Lewiner. Schnyder woods for higher genus triangulated surfaces, with applications to encoding. *Discrete & Computational Geometry*, 42(3):489–516, 2009. `doi:10.1007/s00454-009-9169-z`.

2 Olivier Bernardi and Éric Fusy. Schnyder decompositions for regular plane graphs and application to drawing. *Algorithmica*, 62(3-4):1159–1197, 2012. `doi:10.1007/s00453-011-9514-5`.

3 Therese C. Biedl. Small drawings of outerplanar graphs, series-parallel graphs, and other planar graphs. *Discrete & Computational Geometry*, 45(1):141–160, 2011. `doi:10.1007/s00454-010-9310-z`.

4 Therese C. Biedl. Transforming planar graph drawings while maintaining height. *CoRR*, abs/1308.6693, 2013. `doi:10.48550/arXiv.1308.6693`.

5 Therese C. Biedl. On area-optimal planar graph drawings. In *Proceedings of the 41st International Colloquium on Automata, Languages, and Programming (ICALP)*, volume 8572 of *Lecture Notes in Computer Science*, pages 198–210. Springer, 2014. `doi:10.1007/978-3-662-43948-7_17`.

6 Nicolas Bonichon, Bertrand Le Saëc, and Mohamed Mosbah. Optimal area algorithm for planar polyline drawings. In *Proceedings of the 28th International Workshop on Graph-Theoretic Concepts in Computer Science (WG)*, volume 2573 of *LNCS*, pages 35–46. Springer, 2002. `doi:10.1007/3-540-36379-3_4`.

7 Nicolas Bonichon, Bertrand Le Saëc, and Mohamed Mosbah. Wagner's theorem on realizers. In *Proceedings of the 29th International Colloquium on Automata, Languages and Programming (ICALP)*, volume 2380 of *Lecture Notes in Computer Science*, pages 1043–1053. Springer, 2002. `doi:10.1007/3-540-45465-9_89`.

8 Franz J. Brandenburg. Drawing planar graphs on $\frac{8}{9}n^2$ area. *Electronic Notes in Discrete Mathematics*, 31:37–40, 2008. `doi:10.1016/j.endm.2008.06.005`.

9 Marek Chrobak and Shin-Ichi Nakano. Minimum-width grid drawings of plane graphs. *Computational Geometry*, 11(1):29–54, 1998. `doi:10.1016/S0925-7721(98)00016-9`.

10 Hubert de Fraysseix and Patrice Ossona de Mendez. On topological aspects of orientations. *Discrete Mathematics*, 229(1-3):57–72, 2001. `doi:10.1016/S0012-365X(00)00201-6`.

11 Hubert de Fraysseix, János Pach, and Richard Pollack. How to draw a planar graph on a grid. *Combinatorica*, 10(1):41–51, 1990. `doi:10.1007/BF02122694`.

12 Hristo N. Djidjev and Shankar M. Venkatesan. Reduced constants for simple cycle graph separation. *Acta Informatica*, 34(3):231–243, 1997. `doi:10.1007/s002360050082`.

13 Danny Dolev, Frank Thomson Leighton, and Howard Trickey. Planar embedding of planar graphs. *Advances in Computing Research*, 2:147–161, 1984. URL: `https://hdl.handle.net/1721.1/149047`.

14 Vida Dujmović, Michael R Fellows, Matthew Kitching, Giuseppe Liotta, Catherine McCartin, Naomi Nishimura, Prabhakar Ragde, Frances Rosamond, Sue Whitesides, and David R Wood. On the parameterized complexity of layered graph drawing. *Algorithmica*, 52:267–292, 2008. `doi:10.1007/s00453-007-9151-1`.

15 Stephane Durocher and Debajyoti Mondal. Drawing planar graphs with reduced height. In *International Symposium on Graph Drawing*, pages 392–403. Springer, 2014. `doi:10.1007/978-3-662-45803-7_33`.

16 Stephane Durocher and Debajyoti Mondal. Trade-offs in planar polyline drawings. In *Proceedings of the 22nd International Symposium on Graph Drawing (GD)*, volume 8871 of *LNCS*, pages 306–318. Springer, 2014. `doi:10.1007/978-3-662-45803-7_26`.

17 Stephane Durocher and Debajyoti Mondal. Drawing planar graphs with reduced height. *J. Graph Algorithms Appl.*, 21(4):433–453, 2017. `doi:10.7155/jgaa.00424`.

18 Fabrizio Frati and Maurizio Patrignani. A note on minimum area straight-line drawings of planar graphs. In *Proceedings of the 15th International Symposium on Graph Drawing (GD)*, volume 4875 of *LNCS*, pages 339–344. Springer, 2008. `doi:10.1007/978-3-540-77537-9_33`.

19 Hillel Gazit and Gary L Miller. Planar separators and the Euclidean norm. In *Proceedings of the International Symposium on Algorithms (SIGAL)*, volume 450 of *LNCS*, pages 338–347. Springer, 1990. `doi:10.1007/3-540-52921-7_83`.

20 Md. Iqbal Hossain, Debajyoti Mondal, Md. Saidur Rahman, and Sammi Abida Salma. Universal line-sets for drawing planar 3-trees. In *Proceedings of the 6th International Workshop on Algorithms and Computation (WALCOM)*, volume 7157 of *LNCS*, pages 136–147. Springer, 2012. `doi:10.1007/978-3-642-28076-4_15`.

21 Md Iqbal Hossain, Debajyoti Mondal, Md Saidur Rahman, and Sammi Abida Salma. Universal line-sets for drawing planar 3-trees. *Journal of Graph Algorithms and Applications*, 17(2):59–79, 2013. `doi:10.7155/jgaa.00285`.

22 Charles E. Leiserson. Area-efficient graph layouts (for VLSI). In *Proceedings of the 21st Annual Symposium on Foundations of Computer Science*, pages 270–281. IEEE Computer Society, 1980. doi:10.1109/SFCS.1980.13.

23 Gary L. Miller. Finding small simple cycle separators for 2-connected planar graphs. *J. Comput. Syst. Sci.*, 32(3):265–279, 1986. doi:10.1016/0022-0000(86)90030-9.

24 Debajyoti Mondal, Muhammad Jawaherul Alam, and Md Saidur Rahman. Minimum-layer drawings of trees. In *Proceedings of the 5th International Workshop on Algorithms and Computation*, volume 6552 of *LNCS*, pages 221–232. Springer, 2011. doi:10.1007/978-3-642-19094-0_23.

25 Walter Schnyder. Embedding planar graphs on the grid. In *Proceedings of the 1st Annual ACM-SIAM Symposium on Discrete Algorithms (SODA), San Francisco, California, USA*, pages 138–148. ACM, 1990. URL: http://dl.acm.org/citation.cfm?id=320176.320191.

26 Matthew Suderman. Pathwidth and layered drawings of trees. *International Journal of Computational Geometry and Applications*, 14:203–225, 2004. doi:10.1142/S0218195904001433.

27 Roberto Tamassia, editor. *Handbook of Graph Drawing and Visualization*. CRC Press, 2013.

28 Huaming Zhang. Planar polyline drawings via graph transformations. *Algorithmica*, 57(2):381–397, 2010. doi:10.1007/s00453-008-9215-x.

29 Huaming Zhang and Sadish Sadasivam. On planar polyline drawings. In *Proceedings of the 15th International Symposium on Graph Drawing (GD)*, pages 213–218. Springer, 2007. doi:10.1007/978-3-540-77537-9_22.

30 Xiao Zhou, Takashi Hikino, and Takao Nishizeki. Small grid drawings of planar graphs with balanced bipartition. In *Proceedings of the 4th International Workshop on Algorithms and Computation (WALCOM)*, volume 5942 of *LNCS*, pages 47–57. Springer, 2010. doi:10.1007/978-3-642-11440-3_5.

31 Xiao Zhou, Takashi Hikino, and Takao Nishizeki. Small grid drawings of planar graphs with balanced partition. *Journal of Combinatorial Optimization*, 24(2):99–115, 2012. doi:10.1007/s10878-011-9381-7.